11

The Hydrophobic Topography of Amylose

Abstract: Molecular lipophilicity patterns (MLP's) were calculated for structural models of two polymorphs of amylose. The native double helical and parallel-stranded A-form represents a rather compact structure with an irregular distribution of hydrophilic and hydrophobic regions over the entire outer surface, the interior of the helix is inaccessible even for small molecules. Denaturation yields V-type amylose, which consists out of single-helices with a central channel passing through the molecular axis. In relation to the outside surface the channel is decisively hydrophobic. The hydrophobicity patterns are discussed in regard to the capability of V-amylose to form inclusion complexes with fatty acids. In the well-known dark-blue stained amylose-iodine complex, the channel structure serves as a well-ordered matrix to accommodate nearly linear polyiodide chains with an almost perfect steric fit.

Starch, the biologically most important carbohydrate energy reservoir in plant cells, is contained in the "non-living", but metabolism-associated[471] granules of these cells. Amylose, the unbranched fraction of native starch, is a polymer of several hundred α(1→4)-linked glucose units, which in contrast to the linear chain polymer cellulose composed of β(1→4)-linked glucoses adopts a helical conformation. On the basis of characteristic X-ray diffraction patterns obtained for different samples of starch[472-474], the individual polymorphs were termed A-, B-, C-, and V-("*Verkleisterung*")[473] amylose.

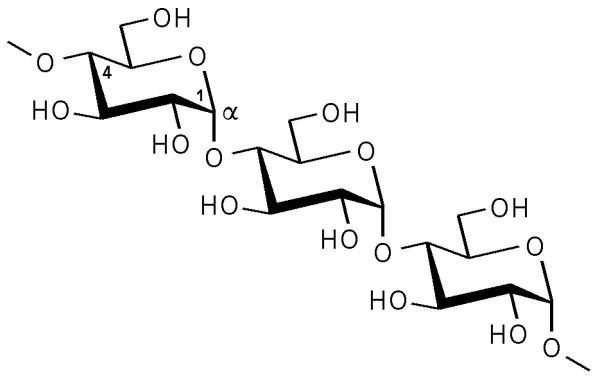

Crystalline Polymorphism of Amylose

Despite the fact, that the glucose residues usually exhibit a rather stiff standard $^4C_1$-conformation, the intersaccharidic linkages are sufficiently flexible, such that the three-dimensional structure of starch[475] strongly depends on the biological origin as well as the way of treatment upon isolation[473,476,477]. In the native form, starch crystallizes in different types A and B, whilst the C-polymorph is a mixture of the former ones[476]. Crystallographic studies[478-481] on these compounds showed the A- and B-forms to be almost identical in their molecular conformations, both differing

mainly in the packing of the helices and the degree of hydration[479], with the B-form being more heavily hydrated than the A-form. The presence of antiparallel packed, right-handed parallel-stranded double helices was proposed for both forms, a model which was subsequently questioned on the basis of biosynthetic as well as computational considerations[482,483].

By joint use of electron diffraction, X-ray powder patterns, fiber diffraction methods, and thorough exploration of systematic absences of reflections in the diffractograms it was unequivocally demonstrated that A-starch crystallizes in the monoclinic space group *B2* containing left-handed parallel-stranded double helices with six glucose residues per turn ($2 \cdot 6 = 12$ sugars units for each turn of the double helix with an axial spacing of approx. 21.4 Å), the asymmetric unit consisting out of a glucotrioside moiety (half turn of each strand). The helices are packed in parallel-fashion as required for this space group, with all hydroxymethyl groups adopting a *gauche-gauche* (*gg*) arrangement[66] relative to the pyranoid rings (*gauche* in relation to the ring oxygen O-5 as well as to C-4)[482].

Denaturation and / or treatment of starch with ethanol[476], isopropanol[484], acetone[484] or DMSO[485] yields V-type amylose[474] in either anhydrous (V_A) or hydrated (V_H) form[486]. Electron diffraction[487,488] and X-ray crystallographic studies[489-491] brought the presence of left-handed single helices with an average pitch of $\approx 8.0 - 8.1$ Å and six glucose residues per turn (6_5-symmetry) close at hand. The mode of helix packing (parallel or antiparallel) still remains a matter of debate[491].

Different conformations were proposed for amylose triacetate (left-handed 14_{11}-helices with 14 glucose moieties in three turns, fiber repeat ≈ 52.53 Å)[492], tri-*O*-ethyl amylose (4_3-helices with a height of ≈ 15.48 Å per turn)[493], and the amylose-KOH complex (6_5-helices, pitch 22.41 Å)[494]. Obviously, the multitude of peculiar structural proposals reflects the difficulties to distinguish multistranded coaxial helices on one side and nested single helices on the other hand, during interpretation fiber diffraction data[495] and demonstrates the dependency of final results on initial molecular models used for refinement[496]. The intramolecular changes during polymorphic transformations of amylose[497] and the conformational stability of V-amyloses and their hydration-induced conversion to the B-type[417] are still subject of discussion: high-resolution solid-state ^{13}C-NMR spectroscopy reached to the conclusion that the occurrence of any drastic conformational changes such as unfolding and refolding during the interconversion of alternative polymorphs seems to be unlikely[417]. It also appeared that B-type amylose consists out of left-handed single helices rather than double helices, which originate from a slight modification of V-amylose only[417]. Despite these serious fundamental problems, the previously

reported similarities between A- and B-amylose[479] and the well-founded double helical solid state structure of the former[482] cannot be ignored and no further speculations should be added.

In solution, alternating well-ordered segmented helices analogous to the crystal geometries and random-coil structures are expected to prevail[498,499]. Thus, both the solid state structures of A-[482] and V_H-type[491] starch were used as molecular images for the local conformational properties[500] of amylose, and thus were entered into a more detailed comparative molecular modeling study.

Molecular Geometries and H-Bonding Patterns of A- and V_H-type Amylose

Molecular models of A-[482] and V_H-amylose[491] were generated according to the X-ray fiber diffraction data, respectively. All hydrogen atoms were positioned geometrically with standard bond lengths of $r_{C\text{-}H} = 1.08$ Å and $r_{O\text{-}H} = 0.90$ Å. Special care was applied to account for hydrogen bonding interactions between hydroxyl groups of appropriate O···O-distances (< 3.2 Å)[328] and OH···O-angles (> 130°). The resulting structures are shown in Fig. 11-1 in a ball and stick-type representation with the molecular contact surfaces[46] – which resemble closely the solvent-accessible surfaces[47] – being superimposed.

In the case of V_H-amylose five single turns ($5 \cdot 6 = 30$ glucose units, $\equiv C_{180}H_{302}O_{151}$) were used, whilst the model of the A-form comprises two turns of the double helix ($2 \cdot 2 \cdot 6 = 24$ glucose units, $\equiv 2 \cdot C_{72}H_{122}O_{61}$), yielding structures of approximately $12 \cdot 12 \cdot 45$ Å in size. In both cases, no intraresidue hydrogen bonding interactions were found within the individual glucose units, but short O-2···O-6-contacts between glucose units of different strands in A-amylose[482] and sugar residues of consecutive helix turns in V_H-amylose[491] are indicative of strong hydrogen bonding networks stabilizing the three-dimensional helical conformations (O···H-distances of approx. 1.9 – 2.1 Å and OH···O-angles around 140 – 160°, cf. Fig. 11-2 and Table 11-1, entries A–D, F). In addition, strong hydrogen bonding between the 3-OH hydroxyl group and the oxygen atom O-2 of adjacent glucose units in V_H-amylose (O···H-distance ≈ 1.94 Å and OH···O-angle close to 180°, Fig. 11-2 and Table 11-1, entry E) strengthens the 2-OH···O-6 interaction by cooperative action[52-54]. These interresidue hydrogen bonds are – in agreement with Jeffrey's systematic analysis of H-bonding patterns in the crystal structures of small carbohydrates[52,140] – energetically more favorable and flexible in geometry (i.e. shorter O···H-distances and larger OH···O-angles) than intraresidue interactions[139]. In consequence, they must be considered as an important factor governing the formation of helical structures in amylose. As was demonstrated for even the solid

state structures of the smaller cyclodextrins, the exact hydrogen bonding pattern may be an individual feature of each crystal of this size and may vary in the course of slight changes in preparation and / or history of the crystals[352]. However, the fundamental types of strong interactions pointed out in this context may be of general validity for amylose crystals.

Several computational studies on the potential energy surface of maltose[13,43,126,501] and analysis of solid state structural data (cf. Table 11-2) revealed only little variations of the intersaccharidic torsion angles Φ (O_5-C_1-O_1-$C_{4'}$) and Ψ (C_1-O_1-$C_{4'}$-$C_{3'}$) between $\alpha(1\rightarrow4)$-linked glucose units (maltose-type linkage): Φ invariably adopts values around $\approx 110 - 120°$ and Ψ is found in the $\approx 120 - 130°$ range (exception: α-phenyl maltoside with $\Psi \approx 101°$).

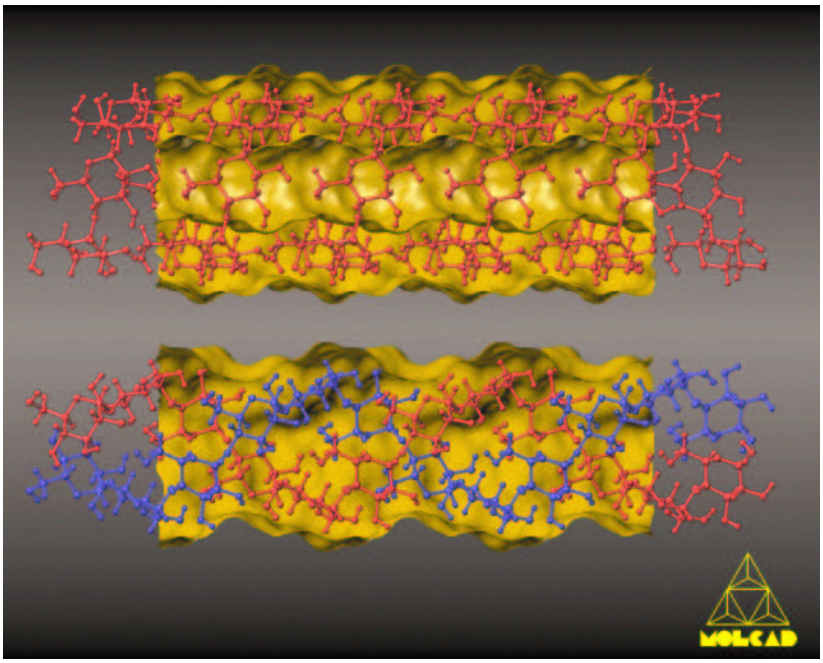

Fig. 11-1. Molecular geometries of V_H-type (*upper* structure) and A-amylose (*lower* entry). Both forms consist out of rod-shaped left-handed helices of $\alpha(1\rightarrow4)$-linked glucose residues with a uniform *gauche-gauche* arrangement[66] of all hydroxymethyl groups in relation to the pyranoid rings throughout. V_H-amylose is single helical (6_5-symmetry), the model comprises five turns of six glucose residues each ($\equiv C_{180}H_{302}O_{151}$, axial spacing of ≈ 8.05 Å per turn). The two individual strands of the double helical A-form ($\equiv 2 \cdot C_{72}H_{122}O_{61}$, two turns with a pitch of ≈ 21.4 Å and 12 glucose units each) were shaded black and white, respectively, to facilitate identification. To exclude "end"-effects for the finite polymer segments of approximately 45 Å length each, the dotted contact surfaces (i.e. the solvent-accessible molecular surfaces) are shown for the center sections of ≈ 30 Å length only.

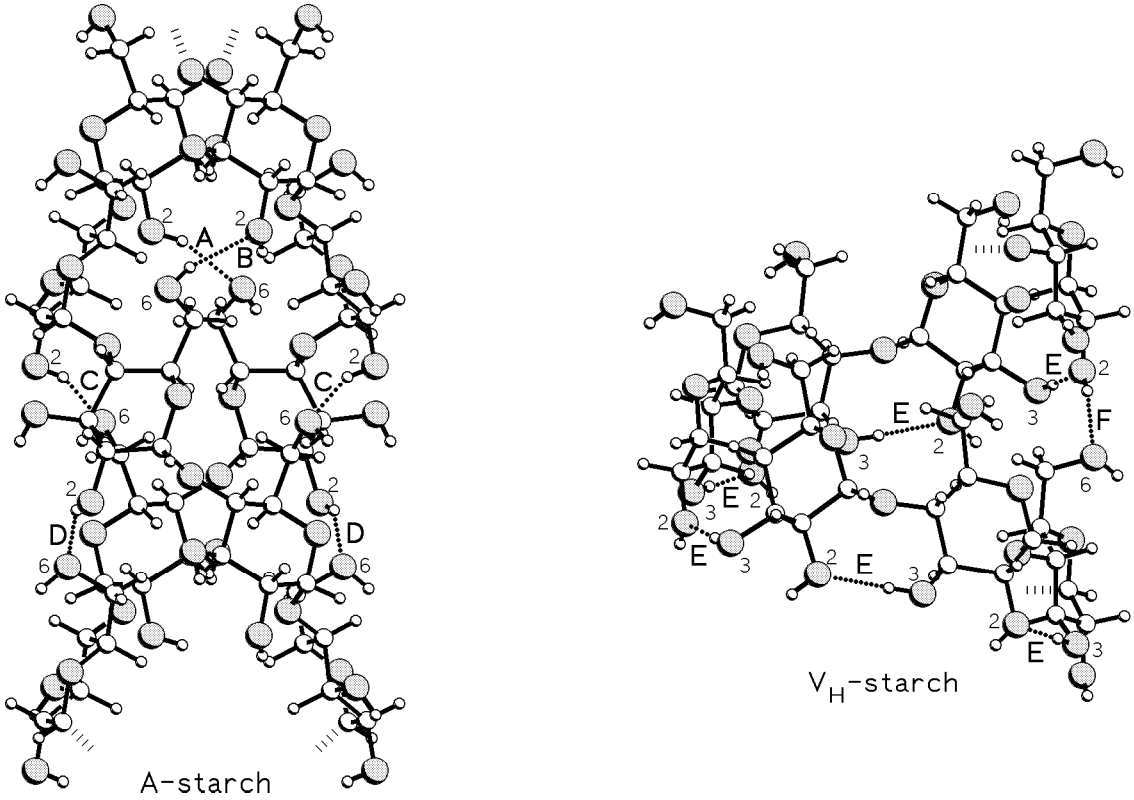

Fig. 11-2. Hydrogen bonding patterns (dotted lines) within the double helices of A-type starch (*left*) and the single helical V_H-type amylose (*right*), calculated from the heavy atom positions of the solid state structures. The letters correspond to different types of hydrogen bonds, the respective geometry parameters are listed in Table 11-1.

Table 11-1. Calculated hydrogen bond geometries (distances and angles) for the A- and V_H-form of amylose. The letters denoting different types of H-bonds correspond to Fig. 11-2.

compound	type of hydrogen bond (cf. Fig. 11-2)		distances [Å] d(O···H)	d(O···O)	angle [°] φ(OH···O)
A-amylose	**A**	2-OH ··· O-6 a)	2.08	2.93	158°
	B	6-OH ··· O-2 a)	2.08	2.93	157°
	C	2-OH ··· O-6 a)	1.90	2.75	156°
	D	2-OH ··· O-6 a)	1.91	2.65	139°
V_H-amylose	**E**	3-OH ··· O-2 b)	1.94	2.84	177°
	F	2-OH ··· O-6 c)	1.95	2.78	154°

a) interstrand hydrogen bonds. – b) H-bond between adjacent glucose units. – c) glucose units one turn apart from each other.

Table 11-2. Mean intersaccharidic torsion angles between α(1→4)-linked glucose units determined from the solid state structures of maltose and its glycosides, cyclodextrins and amylose (root-mean-square deviations in parenthesis).

compound	intersaccharidic torsion angles [a] < Φ >	< Ψ >	ref.
α-maltose	122	133	502
β-maltose	122	133	503
α-phenyl maltoside	109	101	504
β-methyl maltoside	110	129	505
α-cyclodextrin (46 / 54)[b]	107(7)	131 (9)	–[c]
β-cyclodextrin (44 / 50)[b]	111(8)	127 (11)	–[c]
γ-cyclodextrin (9 / 24)[b]	110(4)	129 (4)	–[c]
δ-cyclodextrin (1 / 1)[b]	112(16)	122 (19)	–[c]
(p-NO_2-phenyl glucohexaoside)$_2$·$Ba(I_3)_2$	98(9)	108 (9)	506
V_H-amylose	107	114	491
V_H-amylose iodine / iodide complex	98	119	416
A-amylose	90(3)	88 (1)	482
tri-*O*-acetyl amylose	≈ 82	≈ 85	492
tri-*O*-ethyl amylose	≈ 61	≈ 79	493

a) Φ: O_5-C_1-O_1-$C_{4'}$, Ψ: C_1-O_1-$C_{4'}$-$C_{3'}$. – b) mean values calculated for N_1 different solid state structures of cyclodextrins and inclusion complexes containing N_2 crystallographically independent molecules. – c) Structures contained in the Cambridge Crystallographic Data File[192].

Most notably, the data set provided in Table 11-2 comprises the cyclodextrins – cyclic loop structures consisting of six to nine α(1→4)-linked glucose residues – which in a biomimetic train of thoughts originate from cutting out a turn of the amylose helix and joining the ends. The reverse process – opening the cyclodextrins and elongating the oligosaccharide along a center axis to yield helices – accounts for the differences in Φ and Ψ found for amylose structures (cf. Table 11-2). The changes are minor for the single helices of V_H-starch (Φ ≈ 100 – 110° and Ψ ≈ 115 – 120°) and become more pronouncedly with increasing height of the helix pitch when going to A-amylose (→ Φ ≈ 90°, Ψ ≈ 88°), tri-*O*-acetyl, and tri-*O*-ethyl starch (despite the fact, that there prevail some reservations in respect to the structure determination of the latter amylose derivatives). An analogous trend is observed in the well-resolved solid state structure of a helix-shaped glucohexaoside derivative[506].

Contact Surfaces and Molecular Dimensions of A- and V_H-type Amylose

Because of the increased axial spacing per turn of the helix, the A-form (mean apparent molar volume of $^{\phi}V \approx 155\,Å^3$ per glucose unit) exhibits a more compact molecular geometry than V_H-amylose ($^{\phi}V \approx 160\,Å^3$ / glucose unit). As is already obvious ball and stick type model representation of Fig. 11-1 in conjunction with the dotted contact surface models, the latter form exhibits a central channel passing through the axis of the helix, whilst the interior of the A-form is inaccessible even to small solvent molecules such as water. The molecular dimensions of the two forms of starch become even more clearly evident from cross cut plots (cf. Fig. 6-7) through these surfaces (Fig. 11-3): V_H-amylose exhibits an overall helix diameter of approximately 13.5 Å and a central channel of ≈ 5.4 Å width. Increasing the axial pitch from ≈ 8.1 Å per turn (V_H-form) to approximately 21.4 Å per double turn in A-type amylose requires the helix diameter to decrease to ≈ 10.3 Å only. In consequence, substantial narrowing of interior space leads to the absence of a channel-type structure.

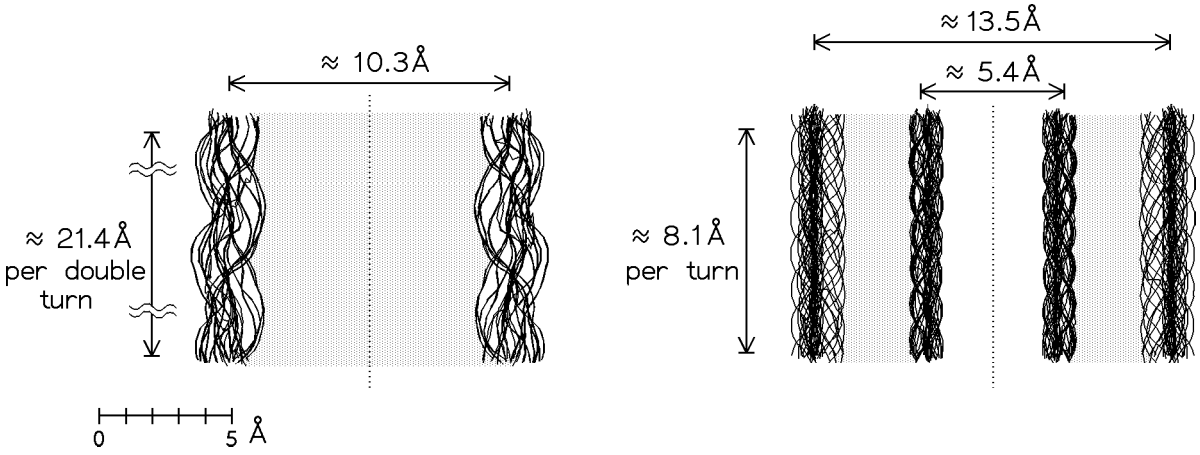

Fig. 11-3. Cross section cuts (cf. Fig. 6-7) through the contact surfaces of A-amylose (*left*) and V_H-amylose (*right*) with a plane through the axis (indicated by dotted lines) of the helices. Contours were obtained from successive 10° rotation steps and superimposed, approximate molecular dimensions are included.

In the solid state structure of the A-form, the water of crystallization is located on places outside the helices only, whilst in V-amylose water occupies positions within the channel, too. In addition, it is a well-established fact that V-amylose is able to form inclusion complexes with long-chain fatty acids[418,419] or small molecules like ozone[507], for example, by incorporation of these compounds into the central channel of the helices.

Molecular Lipophilicity Pattern (MLP) of A- and V_H-type Amylose

In order to obtain an anticipation inasmuch the formation of inclusion complexes of V-amylose is related to hydrophobic interactions, the molecular lipophilicity patterns (MLP's)[58] for the A- and V_H-polymorphs were calculated on the corresponding molecular surfaces (cf. Fig. 11-1) by using the MOLCAD-program[48]. The color-coded visualization[59] of the relative hydrophobicity distribution on these surfaces is shown in Fig. 11-5 for both amylose forms: blue as a reminder of water indicates the most hydrophilic surface regions, whilst the most hydrophobic areas (in relative terms each) are stained yellow-brown.

As apparent from the color-coded representations in Fig. 11-5 – the half opened surface models in the lower picture being particularly lucid in this respect – the hydrophobic characteristics of the V_H-amylose (upper structure each) and the A-form (lower entries) differ significantly, the latter exhibiting an irregular distribution of hydrophobic and hydrophilic surface areas due to the absence of an inner channel. This is distinctively contrasted by the outside surface regions of V_H-amylose, which are highly hydrophilic (blue) while the center channel is decisively hydrophobic (yellow-brown central portion in Fig. 11-5, upper structure in the bottom entry).

In a semi-quantitative way, the percentage distributions of surface portions as a function of their relative hydrophobicity (in arbitrary units) are plotted in Fig. 11-4. For V_H-amylose two independent distributions are found (Fig. 11-4, top), the hydrophilic portion (left side of the abscissa) comprises approximately 72% ($\approx 65\,Å^2$) of the total surface area of $\approx 90\,Å^2$ per glucose unit and is related to the outside surface of the single helix. The second distribution (28%, $\approx 25\,Å^2$ / glucose) is significantly shifted towards the hydrophobic side (right side in Fig. 11-4) and correlates with the inner surface of the channel, in terms of relative hydrophobicity almost no overlap is found between the inside and outside regions. The significantly enhanced hydrophobicity of the channel is caused by the axial O-1 (10% of the inner surface), H-3 (30%), H-5 (25%) as well as the 6-CH_2 (35%) fragments pointing towards the axis of the helix, whilst the outside surface is made up by the H-1, H-2, and H-4 protons, and, most notably, the three hydroxyl groups (2-, 3-, and 6-OH) and the pyranoid ring oxygen (O-5) in similar proportions. The compact structure of A-amylose leads to a decreased surface area of $\approx 75\,Å^2$ / glucose residue only and, in addition, to a uniform bell-shaped distribution of surface portions as a function of hydrophobicity (Fig. 11-4, bottom). The molecular fragments contributing to the outside surface are similar to those of V_H-amylose (*vide supra*) with exception of the 6-CH_2 groups: the methylene grouping, being buried inside the V_H-helix, now contributes to the outside surface area by approx. 7%.

The MLP characteristics of V_H-amylose point towards the hydrophobic effect as an important factor governing the formation of amylose-inclusion complexes with fatty acids by incorporation of the alkyl chains into the hydrophobic channel[418,419]. In contrast to this, the A-form of amylose cannot form such complexes unless substantial widening of the helices takes place to generate a central channel.

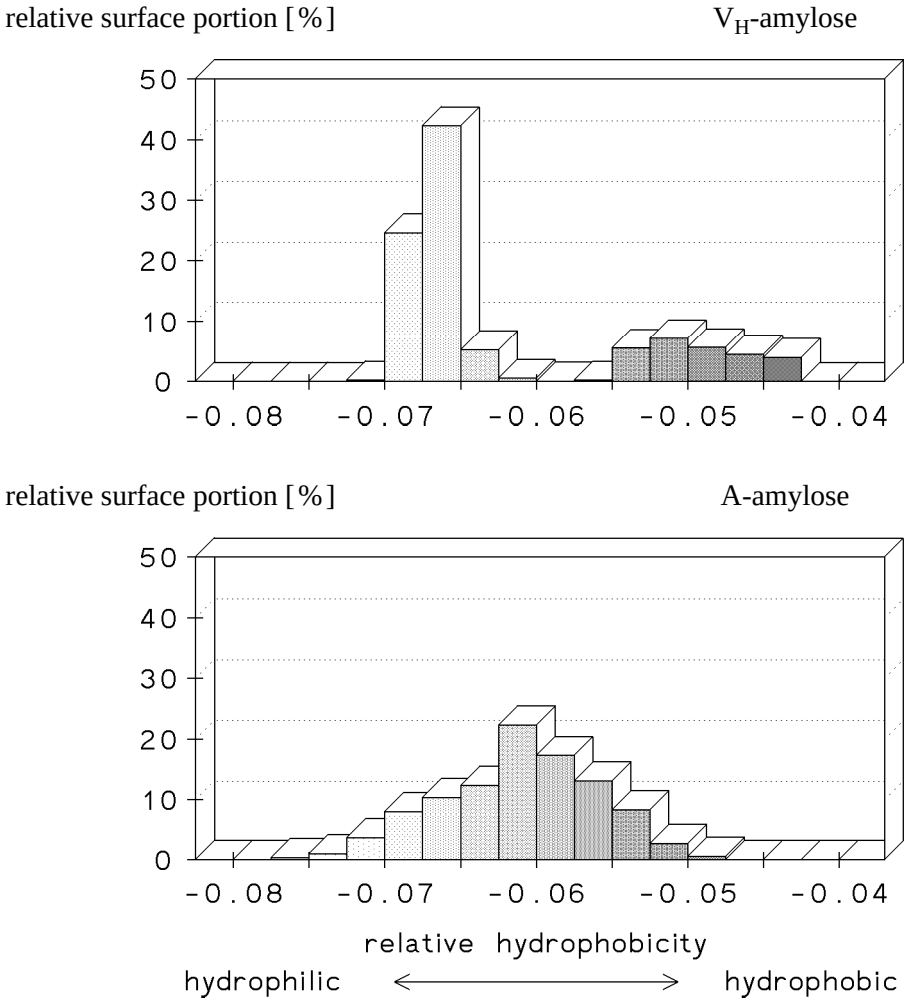

Fig. 11-4. Percentage portions of surface regions (ordinate in relation to the total surface area) as a function of hydrophobicity (abscissa in arbitrary units), calculated for V_H-type amylose (*upper* plot) and the A-form (*lower* diagram). The central channel in V_H-amylose leads to a distinct separation of hydrophilic (outer) and hydrophobic (inner) surface regions with almost no overlap in relative hydrophobicity, whilst for the A-form a uniform bell-shaped distribution is found for the surface portions in relation to their relative hydrophobicity.

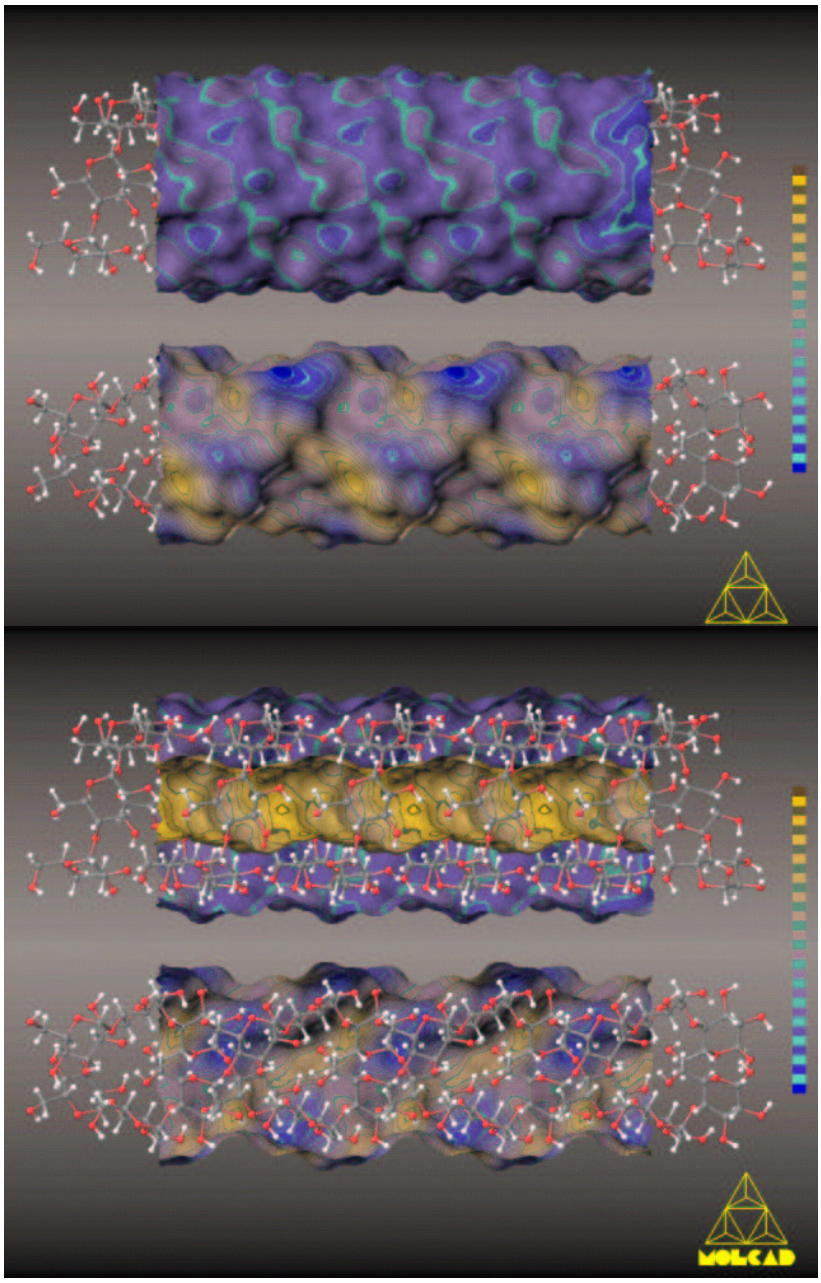
MOLCAD

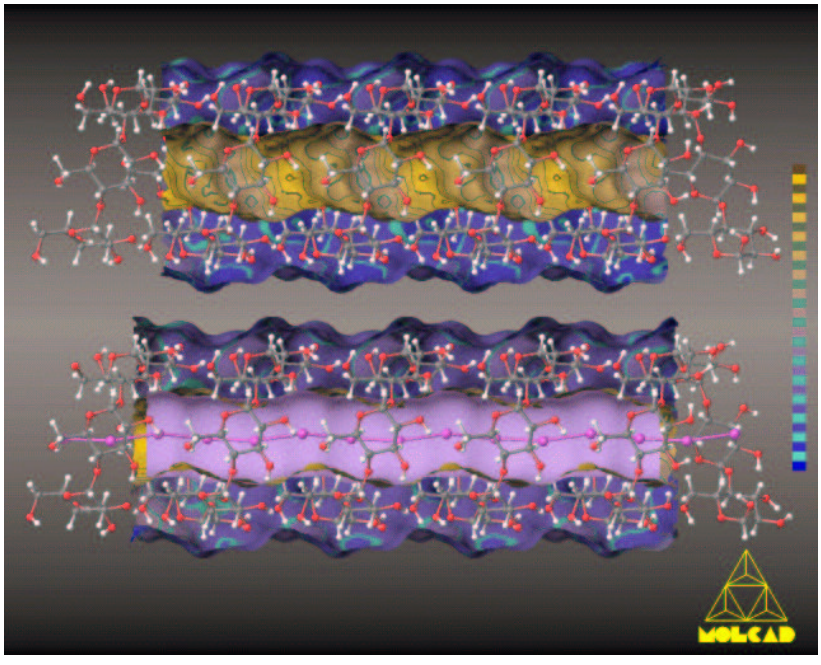
MOLCAD

Fig. 11-5. (opposite page, *top* and *center* picture). Hydrophobic topographies (MLP's) for the amylose fraction of starch: the MLP (blue: hydrophilic surface regions, yellow-brown: hydrophobic areas) on the contact surface of single-stranded V_H-amylose (*upper* structures each) is set against the parallel-stranded double-helical A-form (*lower* model, respectively). In both cases, fragments of approximately 45 Å length are shown, with the surfaces being depicted for the center sections of the rod-shaped polymers only (≈ 30 Å, cf. Fig. 11-1). As evident, the outside surface area of V_H-type amylose appears to be uniformly hydrophilic, as contrasted with the A-form, which is characterized by an irregular distribution of hydrophilic and hydrophobic regions over the entire surface. Whilst A-starch is a rather compact structure lacking cavities accessible for other molecules, the half-opened model of V_H-amylose reveals an essentially hydrophobic (yellow-brown) center channel for this type of starch. It is this almost linear channel which is amenable for the inclusion of fatty-acids by amylose, as well as for the incorporation of iodine / iodide in the well-known deep-blue stained amylose-complex.

The Amylose-Iodine-Iodide Complex

Since its discovery in 1814[508] the nature of the intensely dark-blue stained amylose iodine-complex was subject of numerous investigations[415,416,509-538]. Whilst amylopectin – the branched fraction of starch – only forms instable complexes of purple to red colors[511] and the staining capacity of small glucooligosaccharides with fewer than nine glucose residues is questionable, larger dextrins of 9 – 12 units form yellow-brown complexes. In the range of 12 to 15 sugar residues the color changes from brown to reddish purple and chain lengths of about 18 glucose units are required for the formation of characteristic blue iodine complexes."[517]

In an early fundamental series of papers on the dichroism of flow of starch-iodine solutions, optical properties of crystalline fractions, and X-ray diffraction studies on the starch-iodine complex, Rundle *et al.*[510-512] reached to the conclusion that the iodine linearly line up in the center channel of a six-fold helix.

Fig. 11-6. (opposite page, *bottom* picture). Molecular lipophilicity pattern (MLP) for the starch portion of the V_H-amylose-iodine-iodide complex (*upper* half-opened model according to the solid state structure[416], approximate molecular dimensions cf. Fig. 11-5, blue: hydrophilic surface regions, yellow-brown: hydrophobic areas. For calculation of the MLP the iodine was removed). The hydrophobicity distribution is essentially identical to that of the non-complexed V_H-structure (cf. Fig. 11-5), in particular the pronouncedly hydrophobic channel is clearly obvious. In the *lower* structure, the almost linear iodine chain including its pink-colored contact surface was superimposed to the helix to visualize the perfect steric fit.

Formation of the complex is paralleled by an ordering of loops to form more perfect helices of higher rigidity[518,519] and a slight expansion of the diameter and an increase in length of the cylindrical structure[523]. The maximum uptake of ≈ 30 % (w/w) iodine by amylose[415,524,525] corresponds to a glucose / total iodine ratio of ≈ 2.6 – 2.9[415,525] including approx. 25 % iodide[525].

Incorporation of iodine in organic polymers like amylose is characterized by X-ray diffraction at independent line gratings – straight chains of halogen atoms[513]. The average periodicity of approximately 3.1 Å is substantially invariable of the host lattice[513,514], a fact which was further fortified by optical studies[526] and Mössbauer spectroscopy[527]. The lattice constants are too large for polyhalide chains, but indicate high dipolar interactions[512] and weak metallic properties such as electronic conductivity[528,529], whilst charge transfer processes between amylose and iodide[530] seem unlikely[528]. Clearly, the presence of iodine as well as iodide[531] in aqueous[415,529,532] solutions is a mandatory prerequisite for the formation of the blue complex and binding occurs in a cooperative way[533,534] by slow formation of stable I_{11}^{3-} nuclei inside the helices and rapid linear propagation[533]. With increasing iodide concentration the bluing species (polymeric unit of approx. $(C_6H_{10}O_5)_{16.5}\cdot I_6$[535]) seems to change from I_{10}^{2-} to I_8^{2-} and I_6^{2-}[536,537], simultaneously shifting the maximum absorption towards lower wave lengths[531a]. The enthalpy of the amylose / iodine interaction is rather large with -50 – -90 kJ/mol molecular iodine bound[538].

In summary, all this data points towards the solid state structure of the amylose-iodine complex derived from X-ray fiber diffraction analysis[416] – albeit the low resolution of the structure refinement – to represent a good model for the inclusion complex even in aqueous solution: an almost linear I_3^- polyiodide chain with I···I-separations of ≈ 2.91, 2.91 and 2.99 Å, respectively, was found, unfortunately the actual length of the iodine chains could not be determined. The fiber repeat of the amylose helix of ≈ 8.17 Å is slightly increased when compared to that of iodine-free V_H-amylose (≈ 8.05 Å) and is incongruous with the iodine repeat distance.

According to the methodology outlined above, the hydrophobic characteristics of the amylose-iodine complex were calculated for the solid state conformation[416]. In Fig. 11-6, the MLP of the host helix itself – except the slightly increased (≈ 1.5 %) pitch per turn its conformation is essentially identical to the V_H-amylose depicted in Fig. 11-5 – is shown in color-coded form on the corresponding contact surface (upper structure), the iodine has been removed for calculation of the MLP. It is the pronouncedly hydrophobic central channel of this structure, which serves as a matrix for incorporation and alignment of the iodine species. Superimposition of the amylose

helix with the iodine chain – including its pink-colored contact surface (Fig. 11-5, bottom structure) – clearly demonstrates the perfect steric fit. The almost ideal guest-host relationship, the nearly perfect linear arrangement of iodine / iodide in channels – not of infinite length, but long enough to include several consecutive polyiodide units – imposes the unique features and the deep-blue color to the complex.

Cyclodextrins – torus-shaped single-turn analogs of starch exhibiting a hydrophobic central cavity – are also able to form inclusion complexes with iodine, which in the case of α-CD (six glucose units) are deep-blue colored, for β-CD (seven glucoses) the complex becomes less stable and brown-colored, whilst for γ-CD (eight residues) no formation of an inclusion complex was observed[539]. The torus-shape of ≈ 8.0 Å height only causes a characteristic MLP topography: the wider truncated cone aperture of the cyclodextrins made up by all secondary 2- and 3-OH groups of the glucose residues is distinctly hydrophilic, whilst the narrower opposite rim of the primary 6-CH_2OH is hydrophobic. In the solid state structures[318] of cyclodextrin inclusion complexes with iodine[410,411] and polyiodide[405,412-414] herringbone-type arrangements or infinite channels are formed by adjacent cyclodextrins cavities. In all cases, the alternating hydrophobicity patterns in the direction parallel to the channel axis are retained, and thus devaluate the model character of the cyclodextrins for the amylose-iodine complex, the observation of different colors for these compounds represents a fortification of this fact. High resolution crystal structure analysis of the brown-colored (*p*-nitrophenyl glucohexaoside)$_2 \cdot Ba(I_3)_2$ complex revealed an anti-parallel double helix formed by two oligosaccharide strands[506], and the structural differences to the amylose-iodine complex are striking.

Obviously, the hydrophobic center channel of V_H-amylose provides a unique environment to accommodate iodine and fix it in a linear arrangement. The MLP's presented above for the non-complexed as well as for the complexed polymorphs of starch represent a further step towards the visual perception of the physico-chemical properties of these polymers and provide new insights into prevailing structural intricacies. Last but not least, these representations are of characteristic aesthetic value, such that the perception of theoretical principles is greatly facilitated.